Chinese Journal of Chemical Engineering 69 (2024) 220–226

Contents lists available at ScienceDirect

Chinese Journal of Chemical Engineering

journal homepage: www.elsevier.com/locate/CJChE

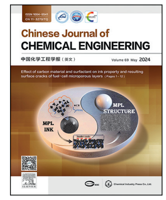

Full Length Article

Supersonic expansion and condensation characteristics of hydrogen gas under different temperature conditions

Xinyue Duan [1], Zeyu Zhang [2], Ziyuan Zhao [2], Yang Liu [2], Liang Gong [1], Xuewen Cao [2], Jiang Bian [2,*]

[1] *College of New Energy, China University of Petroleum (East China), Qingdao 266580, China*
[2] *College of Pipeline and Civil Engineering, China University of Petroleum (East China), Qingdao 266580, China*

ARTICLE INFO

Article history:
Received 19 October 2023
Received in revised form
16 December 2023
Accepted 21 December 2023
Available online 7 February 2024

Keywords:
Hydrogen
Liquefaction
Supersonic
Condensation
Laval nozzle
Computational fluid dynamics

ABSTRACT

This paper introduced supersonic expansion liquefaction technology into the field of hydrogen liquefaction. The mathematical model for supersonic condensation of hydrogen gas in a Laval nozzle model was established. The supersonic expansion and condensation characteristics of hydrogen gas under different temperature conditions were investigated. The simulation results show that the droplet number rises rapidly from 0 at the nozzle throat as the inlet temperature increases, and the maximum droplet number generated is 1.339×10^{18} kg^{-1} at inlet temperature of 36.0 K. When hydrogen nucleation occurs, the droplet radius increases significantly and shows a positive correlation with the increase in the inlet temperature, and the maximum droplet radii are 6.667×10^{-8} m, 1.043×10^{-7} m, and 1.099×10^{-7} m when the inlet temperature is 36.0 K, 36.5 K, and 37.0 K, respectively. The maximum nucleation rate decreases with increasing inlet temperature, and the nucleation region of the Laval nozzle becomes wider. The liquefaction efficiency can be effectively improved by lowering the inlet temperature. This is because a lower inlet temperature provides more subcooling, which allows the hydrogen to reach the thermodynamic conditions required for large-scale condensation more quickly.

1. Introduction

The massive greenhouse effect caused by the massive use of primary energy has become a common concern worldwide [1]. Decarbonization and energy transition will play an important role in future energy and environmental systems. Hydrogen energy has a wide range of sources, storage, and regeneration capabilities [2]. With its high calorific value of combustion and electrification, as well as being nonpolluting, hydrogen energy is generally recognized as a clean and efficient secondary energy source in the international energy arena. There are currently two main methods of hydrogen storage in the world [3]: high-pressure gaseous and low-temperature liquid. In terms of storage density and capacity, the density of liquid hydrogen at atmospheric pressure is as high as $70.9\ kg \cdot m^{-3}$, which is equivalent to 1.8 times the density of gaseous hydrogen at 7×10^7 Pa. Low-temperature liquid hydrogen storage has significant advantages.

At present, hydrogen liquefaction mainly involves transplanting traditional natural gas liquefaction processes. However, due to the fact that the temperature required for hydrogen liquefaction is much lower than that of natural gas, more cumbersome cryogenic processes need to be set up, resulting in complex processes, high equipment requirements, large land occupation, and high investment costs, which have become a technical bottleneck restricting the development of the hydrogen energy industry [4].

Supersonic expansion liquefaction technology is an efficient technology in the field of liquefaction in recent years and is now widely used in natural gas deacidification, deheavy hydrocarbons, and offshore natural gas liquefaction [5]. Compared to conventional machining, this new machine has no moving parts, which ensures its high reliability and availability [6]. This technology works on the principle that hydrogen enters the Laval nozzle through a nozzle, where the velocity of the hydrogen increases dramatically due to the decompression and expansion effects of the Laval nozzle, while

* Corresponding author.
E-mail address: bj@upc.edu.cn (J. Bian).

https://doi.org/10.1016/j.cjche.2023.12.024
1004-9541/

the temperature decreases dramatically, thus liquefying the hydrogen. The introduction of supersonic expansion liquefaction technology into the field of hydrogen liquefaction will help to simplify the traditional process and increase the efficiency of liquefaction [7].

The mechanization of supersonic expansion and condensation in Laval nozzles has been studied by many scholars. Frankl [8] explained the flow characteristics at the intersection of the transition line and the axis of symmetry (center of the nozzle). Chen *et al.* [9–11] illustrated the possibility of using supersonic technology to capture carbon dioxide from flue gas and suggests a potential method for reducing greenhouse gas emissions. Liu *et al.* [12,13] studied the differences in internal flow patterns caused by different Laval nozzle structures and applied the equation to determine the location of surge generation in the nozzle. Pathak *et al.* [14] investigated the condensation characteristics of deuterium oxide and nonane vapors in the nozzle. Bian *et al.* [15,16] analyzed the condensation mechanism of carbon dioxide and hydrogen sulfide mixed components in natural gas. They proposed a technical route to remove mixed sour gas by the ultrasonic liquefaction method, obtained the in-jet pipe condensation pattern, and verified it experimentally. Cao *et al.* [17,18] established a mathematical model for the spontaneous condensation of a two-component single condensable gas, studied the influence of the strength and structural characteristics of the cyclonic field on the supersonic cyclonic separation efficiency. On this basis, they established a mathematical model for the supersonic condensation of hydrogen sulfide in natural gas and studied the nucleation law of acid gas in the nozzle. Chen *et al.* [19] analyzed the effect of excitation waves on carbon dioxide nucleation and droplet growth in the Laval nozzle. Liu *et al.* [20] analyzed the effect of the nozzle pressure ratio n on the air jet field. Yang *et al.* [21] analyzed the spontaneous condensation mechanism of water vapor in Laval nozzles by building computational fluid dynamics models in Ansys-Fluent software.

Although scholars have conducted extensive research on the condensation characteristics of supersonic flow in nozzles, most of these studies focus on water vapor or acid gas components. To our knowledge, no one has studied the condensation characteristics of hydrogen gas. In this paper, to verify the feasibility of applying supersonic expansion liquefaction technology to the field of hydrogen liquefaction, mathematical models for single-component nucleation and condensation were established and the supersonic flow and condensation characteristics of hydrogen inside Laval nozzles was studied, the influence of inlet pressure on the variation in hydrogen condensation parameters in Laval nozzles was systematically analyzed.

2. Structure Design

The Laval nozzle can be divided into a subsonic decompression section [22], a throat section to reach the speed of sound, and a supersonic expansion section according to the hydrodynamic properties, as shown in Fig. 1. To reduce the degree of turbulence in the inlet stream and improve flow stability, an inlet section is required before the decompression section [23,24]. A flow path of contraction followed by expansion is used to ensure that pressure changes can meet condensation conditions. Table 1 shows the detailed dimensions.

Hydrogen is accelerated to reach the speed of sound in the nozzle tapering section to complete the expansion and compression process, in order to maintain the stability of the gas flow and to avoid disturbances, the Witoszynski curve [25] is used to form the structure of the nozzle tapering section, and its curve satisfies the following equation:

$$R=\frac{r_{\rm cr}}{\sqrt{1-\left[1-\left(\frac{r_{\rm cr}}{r_1}\right)^2\right]\frac{\left(1-\frac{x^2}{L^2}\right)^2}{\left(1+\frac{x^2}{3\times L^2}\right)^3}}} \tag{1}$$

3. Model Building

3.1. Governing equations

The heat transfer coefficient of droplets in steam is related to the droplet size and the relative velocity of droplets in the vapor molecule. The droplet radius is very small (approximately 10^{-9} m), so the slip velocity between the vapor and liquid droplets is ignored. Hydrogen is a single-component compressible gas that flows in a Laval nozzle while undergoing energy changes, and the governing equations involved are the continuity, momentum, and energy equations [26]:

Continuity equation:

$$\frac{\partial\rho}{\partial t}+\frac{\partial}{\partial x_i}(\rho u_j)=S_{\rm m} \tag{2}$$

Momentum equation:

$$\frac{\partial}{\partial t}(\rho u_i)+\frac{\partial}{\partial x_j}(\rho u_i u_j)+\frac{\partial}{\partial x_j}-\frac{\partial\tau_{ij}}{\partial x_j}-\frac{\partial{\tau_{ij}}^{-1}}{\partial x_j}=S_{\rm u} \tag{3}$$

Table 1
Parameters of the Laval nozzle

Parameters	Value/mm
Length of the entry section	85.00
Length of the tapered section	238.00
Length of the expanding section	238.00
Inlet diameter	136.00
Diameter of nozzle throat	17.00
Diameter of the outlet	20.00

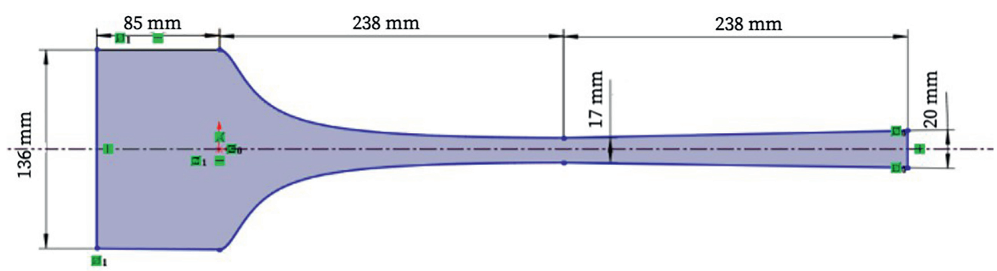

Fig. 1. Laval nozzle construction diagram.

Energy equation:

$$\frac{\partial}{\partial t}(\rho E)+\frac{\partial}{\partial x_i}(\rho u_j E+u_j p) -\frac{\partial}{\partial x_j}\left(u_i\tau_{ij}+u_i\tau_{ij}^{-1}\right)+\frac{\partial}{\partial x_j}\left(q_j+q_j^{-1}\right)=S_{\rm h} \tag{4}$$

The source terms are added in the above equations to consider the influence of the phase change process, presented as Eqs. (5)–(7):

$$S_{\rm m}=-m_{\rm v} \tag{5}$$

$$S_{\rm u}=-m_{\rm v}u \tag{6}$$

$$S_{\rm h}=-m_{\rm v}(h-h_{\rm lv}) \tag{7}$$

The continuity equation of the liquid phase and the relations between droplet radius, droplet number, and mass fraction of liquid phase are as follows:

$$\frac{\partial}{\partial t}(\rho_{\rm v}N)+\frac{\partial}{\partial x_j}(\rho_{\rm v}u_jN)=J \tag{8}$$

$$\frac{\partial}{\partial t}(\rho_{\rm v}N)+\frac{\partial}{\partial x_j}(\rho_{\rm v}u_jN)=J \tag{9}$$

$$r_{\rm d}=\left(\frac{3Y}{4\pi\rho_{\rm l}N}\right)^{\frac{1}{3}} \tag{10}$$

3.2. Nucleation and droplet growth model

The nucleation rate of water vapor was calculate by the internally consistent classic nucleation theory (ICCT) model [12], which can be calculated as:

$$J_{\rm ICCT}=\frac{1}{S}\frac{{\rho_{\rm v}}^2}{\rho_l}\sqrt{\frac{2\sigma}{\pi m_{\rm o}^3}}\exp\left[-\frac{16\pi}{3}\frac{\sigma^3}{k_{\rm B}{\rho_{\rm l}}^2R_{\rm M}^2T^3(\ln S)^2}\right]\exp\theta \tag{11}$$

According to the Gyarmathy droplet growth model [27], the heat transfer coefficient between the hydrogen molecule and the condensed droplet, Kr, can be derived as:

$$Kr=\frac{\lambda_{\rm v}}{r}\frac{1}{1+\frac{2\sqrt{8\pi}}{1.5\,Pr_{\rm v}}\frac{\gamma}{\gamma+1}Kn} \tag{12}$$

The droplet growth rate equation is derived as:

$$\frac{{\rm d}r}{{\rm d}t}=\frac{\lambda_{\rm v}\left(1+\frac{r_{\rm c}}{r}\right)(T_{\rm s}-T)}{\rho_l h_{{\rm v}l}\left(r+\frac{\sqrt{8\pi}}{1.5\,Pr_{\rm v}}\frac{\gamma}{\gamma+1}\bar{l}\right)} \tag{13}$$

3.3. Numerical model

The fluid simulation software Ansys-Fluent can be used to simulate and study the fluid in a specific flow field. For the supersonic flow characteristics of hydrogen in the nozzle, the semi-implicit method for pressure-linked equation algorithm can be used for the coupled velocity and pressure calculation [28]. In the simulation of the Reynolds stress term, the turbulent viscosity coefficient method can be used. The standard k–ω model is a turbulence model suitable for compressible and wall-constrained flow calculations [29] and is particularly suitable for the case of spinless flow conditions.

According to the flow characteristics of the supersonic compressible gas, the inlet and outlet boundary conditions are set for the interior of the nozzle. In this paper, the inlet boundary condition is determined as a pressure inlet, while the total pressure, static pressure, total temperature, and turbulence parameters need to be specified [30]. The outlet boundary condition is set at the pressure outlet, and all flow parameters are not set, as they are calculated by Fluent software [31]. In addition, to ensure the accuracy of the simulation results, a slip-free, seepage-free, adiabatic boundary was used to simulate the solid wall [32].

The calculations require dynamic monitoring of residuals and outlet mass flow rate variations. It should be noted that the calculations are considered to have converged when the residuals of the energy equation are below 10^{-6}, the residuals of the residual equation are below 10^{-3}, and the relative errors of the outlet and inlet mass flow rates are below 0.05% [33]. The specific settings are listed in Table 2.

3.4. Grid independence and verification

The mesh of the nozzle needs to be divided and the quality of its mesh needs to be verified to evaluate the effect of meshing on the simulation results. The inlet temperature was set at 36.5 K and the inlet pressure at 1.05×10^6 Pa, and grid numbers 6006, 11914, 21358, and 32218 were selected to simulate the temperature drop in the Laval nozzle. The degree of curve stacking is higher when the grid number is 21358 or above. The accuracy of the calculation is better in this case. Therefore, grid number 21358 is chosen for comprehensive consideration. Moses's experimental data [34] were used to verify the numerical methods discussed above. The

Table 2
Numerical setting

Numerical scheme	Numerical setting
Numerical computational platform	Ansys Fluent 19.2
Secondary development platform	Visual studio 2017
Solver type	Density-based
Turbulence model	(SST) k–ω model
Equation of state	Peng-Robinson real gas equation
Third-party link library	NIST REFPROP
Boundary condition	Pressure and temperature inlet: 1.05×10^6–1.15×10^6 Pa, 36 K–37 K Wall: No slip and thermal isolation Hydrogen mole fraction: 100%
Convergence criteria	Net relative error in mass flow rate is less than 10^{-6}

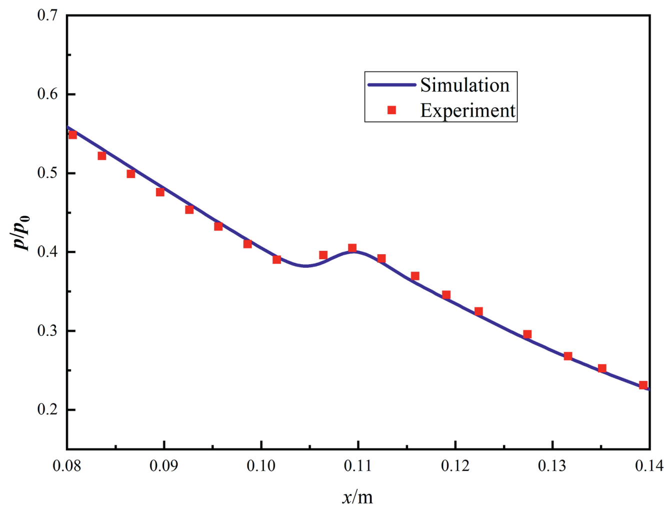

Fig. 2. Verification results.

experimental medium was water vapor. The pressure ratio distribution on the axis of the nozzle was measured in the experiment. The experimental and numerical results are presented in Fig. 2. As shown, the condensation process is accurately captured and the numerical results agree with the experimental results well, which shows that the mathematical model and numerical method can be used to simulate the spontaneous condensing flow of gas in the Laval nozzle.

4. Hydrogen Supersonic Flow Characteristics

The Laval nozzle plays a crucial role in the hydrogen expansion refrigeration and condensation process, and the low temperature environment it generates provides the necessary conditions for hydrogen condensation. To characterize the nozzle cooling effect, the effect of inlet pressure on nozzle cooling was analyzed by keeping the inlet temperature constant at 36.5 K and varying the inlet pressure to 1.05 $\times$ 10^6 Pa, 1.10 $\times$ 10^6 Pa, and 1.15 $\times$ 10^6 Pa, respectively, and the simulation results are shown in Fig. 3 below; the inlet temperature was set to 36.0 K, 36.5 K, and 37.0 K by keeping the inlet pressure constant at 1.10 $\times$ 10^6 Pa and distributing the effect of inlet temperature on the cooling effect of the nozzle is analyzed, and the simulation results are shown in Fig. 4.

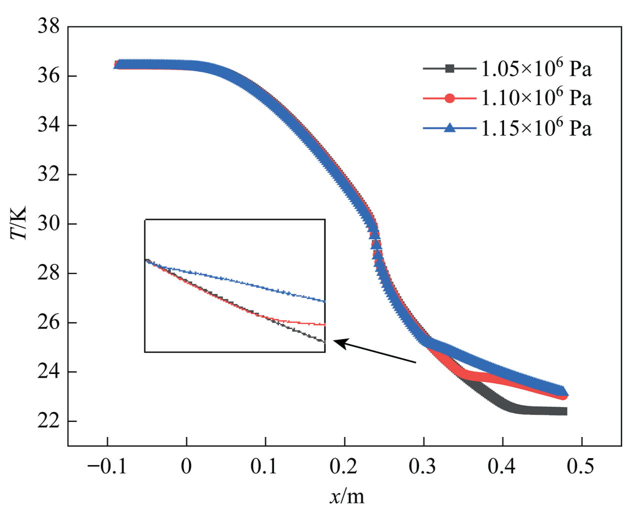

Fig. 3. Results of the temperature drop along the axis at different inlet pressures.

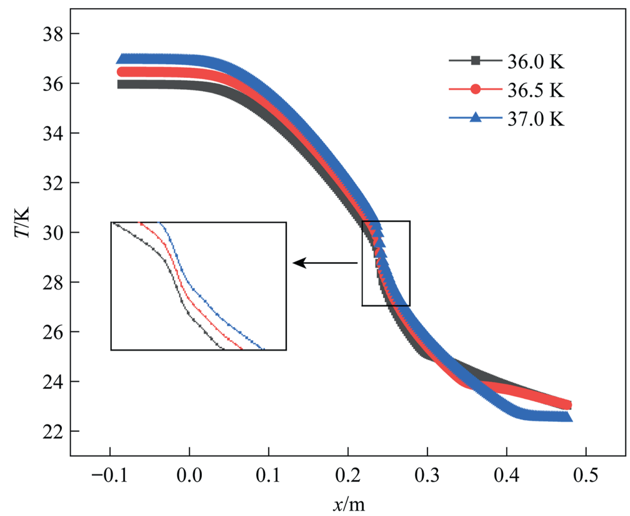

Fig. 4. Results of the temperature drop along the axis at different inlet temperatures.

According to the simulation results in Figs. 3 and 4, the hydrogen temperature does not change in the inlet section of the Laval nozzle and starts to decrease at a certain position in the tapering section. Since condensation gives off some heat, the temperature increases slightly and then decreases in the tapering section, but overall, the temperature still decreases, and finally, the temperature reaches a minimum value at the exit of the tapering section.

5. Supersonic Expansion Condensation Properties of Hydrogen Gas

To investigate the condensation characteristics of hydrogen molecules at different temperatures in the nozzle, the inlet pressure was kept constant at 1.10 $\times$ 10^6 Pa, and the inlet temperatures varied to 36.0 K, 36.5 K, and 37.0 K to study the distribution of six key parameters in the nozzle: droplet number, liquid phase mass fraction, droplet growth rate, droplet radius, nucleation rate, and subcooling. The results are shown in Fig. 5–Fig. 10.

According to the simulation results in Fig. 5, the droplet number decreases with increasing inlet temperature, and at an inlet temperature of 36.0 K, the droplet number rises rapidly from 0 to 1.339 $\times$ 10^{18} kg^{-1} at the location of the Laval nozzle throat, but the droplet number generated at 36.5 K and 37 K are smaller, 1.929 $\times$ 10^{17} kg^{-1} and 6.089 $\times$ 10^{17} kg^{-1}, respectively. According to Fig. 6, the liquid phase mass fraction decreases from 11.539% to

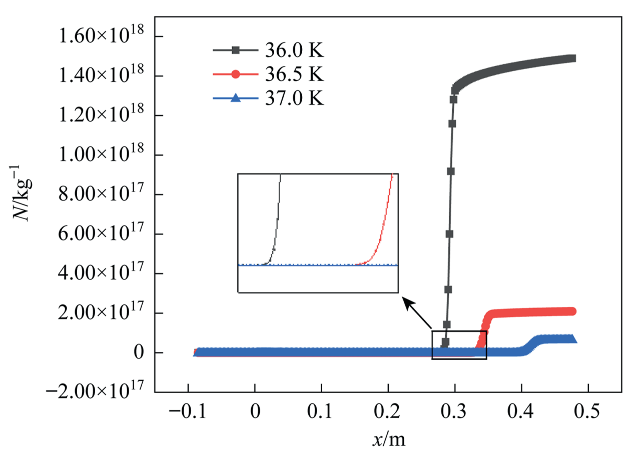

Fig. 5. Changes in droplet number.

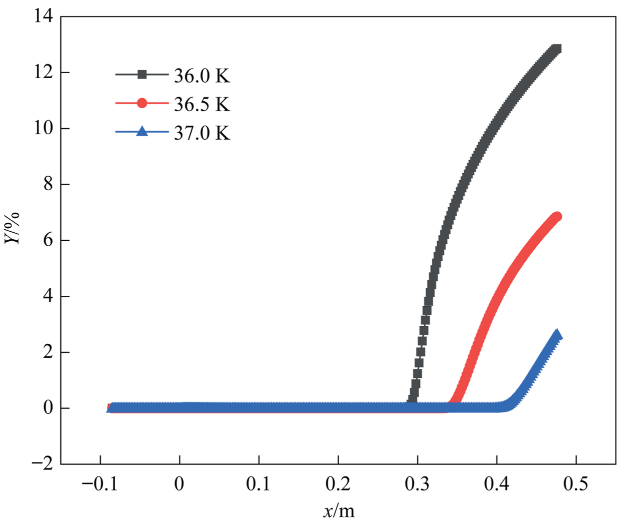

Fig. 6. Variations of mass fraction of liquid phase.

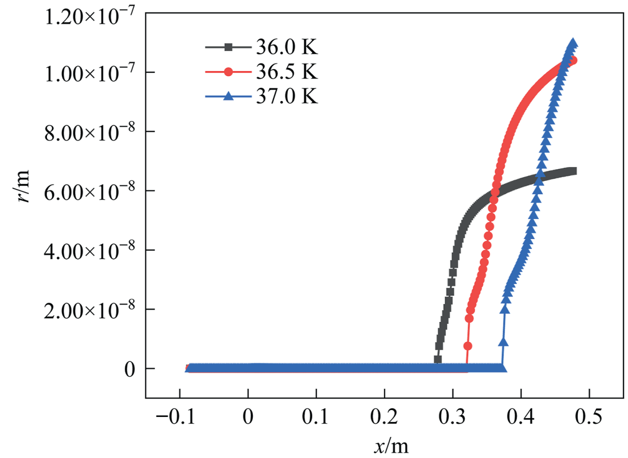

Fig. 8. Variations of droplet radius.

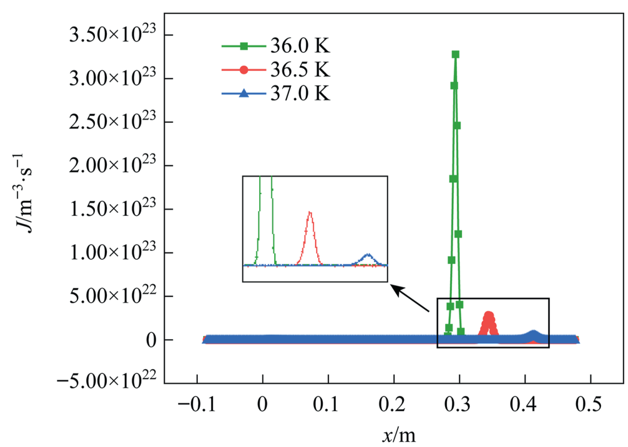

Fig. 9. Changes in nucleation rate.

1.419% as the inlet temperature increases from 36.0 K to 37.0 K. The results show consistency with the trend of droplet number change.

According to Fig. 7, with the increase in inlet temperature from 36.0 K to 37.0 K, the droplet growth rate changes abruptly from 0 to the maximum value in a short distance and then decreases rapidly. This change is mainly because at the early stage of nucleation, the number of nuclei is small and the droplet growth rate is fast, with the peak values of droplet growth rate at three inlet temperatures being 9.208×10^{-4} $m\cdot s^{-1}$, 1.125×10^{-3} $m\cdot s^{-1}$, and 1.403×10^{-3} $m\cdot s^{-1}$. The nucleation rate increases sharply at the later stage of nucleation, and the latent heat is released during the droplet formation process so that the condensation rate of the vapor gradually decreases and the evaporation rate of the droplet gradually increases. As the inlet temperature of the Laval nozzle decreases, the maximum droplet growth rate increases at the beginning of nucleation, but then the droplet growth rate decreases more rapidly, resulting in a decrease in the average droplet growth rate.

The droplet radius distributions in the Laval nozzle are shown in Fig. 8. No droplets are generated when hydrogen first enters the Laval nozzle, and the fluid component is completely in the gas phase; after nucleation occurs, the droplet radius increases and gradually increases with increasing inlet temperature, and when the inlet temperature is 36.0 K, 36.5 K, and 37.0 K, the maximum droplet radii are 6.667×10^{-8} m, 1.043×10^{-7} m, and 1.099×10^{-7} m. At the same time, the condensation position moves away from the throat as the inlet temperature increases, from $x = 0.284$ m to $x = 0.388$ m. This is because the higher the inlet temperature is, the greater the subcooling required for gas condensation, and condensation is less likely to occur.

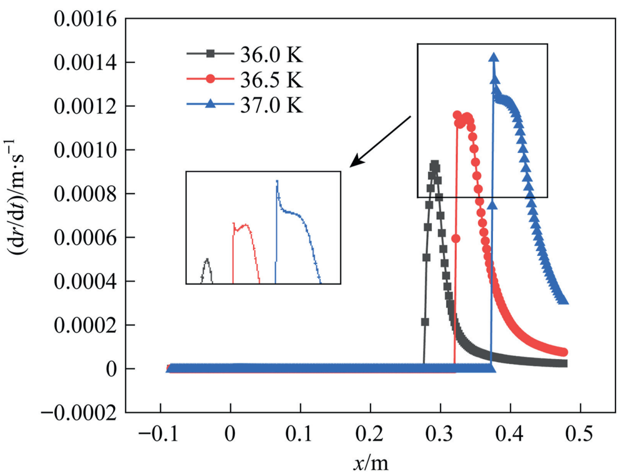

Fig. 7. Variations of droplet growth rate.

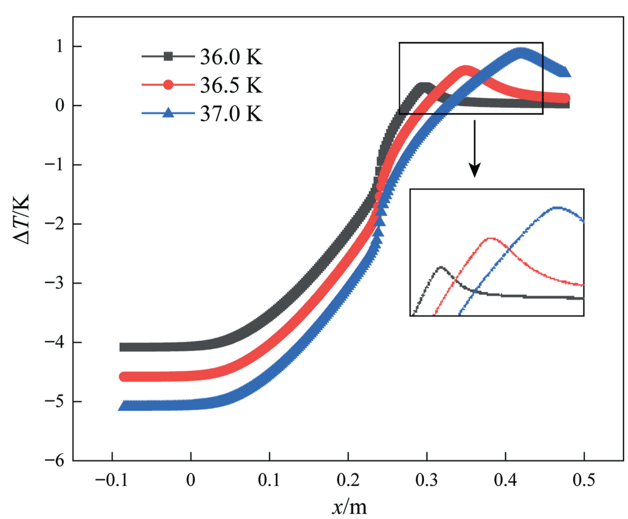

Fig. 10. Changes in subcooling degree.

According to Fig. 9, the maximum nucleation rate decreases with increasing inlet temperature, reaching a maximum value of 3.278×10^{23} $m^{-3}\cdot s^{-1}$ at $x = 0.294$ m when the temperature is 36.0 K, and when the temperature increases to 37.0 K, the nucleation rate reaches a maximum value of 2.028×10^{22} $m^{-3}\cdot s^{-1}$ at $x = 0.412$ m. In addition, the nucleation region of the Laval nozzle becomes wider as the inlet temperature increases.

According to Fig. 10, the position where the hydrogen subcooling reaches its peak at lower inlet temperatures is shifted forward due to the widening of the radius of the condensed droplets, which leads to more droplets condensing out of the gas phase, thus increasing the mass fraction of the liquid phase, and when the inlet temperature decreases from 37 K to 36 K, the higher the subcooling of the gas inlet at lower inlet temperatures can reach the subcooled state earlier, and at the same time, the starting position of nucleation is also moved forward.

6. Conclusions

This paper aims to investigate the characteristics of liquefied hydrogen in a supersonic nozzle, an in-depth study utilizing theoretical analysis and numerical simulations to design the structure of the supersonic nozzle was carried out and carry out, the flow and condensation characteristics of hydrogen gas in the nozzle was numerically simulated. The main findings of this paper are as follows.

(1) Decreasing the inlet temperature increases the gas inlet subcooling, resulting in a forward shift in the onset of condensation, an increase in droplet size, more gas components condensing into the liquid phase, and a more significant liquefaction effect from the Laval nozzle.
(2) As the inlet temperature increases, condensation will migrate further away from the nozzle inlet. At the same time, the nucleation rate and droplet number decrease. The liquefaction effect of the Laval nozzle is reduced.
(3) The gas enters the inlet section of the Laval nozzle and begins to drop in temperature in the tapering section, and the temperature drops significantly by the time it reaches the throat position, by approximately 2 K. The temperature drop decreases after the gas enters the tapering section and continues to cool.
(4) After the hydrogen gas enters the Laval nozzle, the high-speed flow of the gas stream causes a low-temperature effect, and the low-temperature environment promotes the condensation of hydrogen. As the inlet pressure increases and the inlet temperature decreases, the cooling efficiency inside the nozzle is significantly enhanced.
(5) Gas supersaturation remains high until nucleation. In the tapering section of the nozzle, the gas is in a state of extreme disequilibrium, which leads to the appearance of condensation nuclei. The nucleation process was of short duration, and the number of nuclei was large, with a maximum nucleation rate of 3.278×10^{23} $m^{-3}\cdot s^{-1}$. The gas nucleation rate decreased significantly at the end of nucleation.

The above results have some guiding significance for the application of supersonic liquefaction technology in practical engineering. In view of the high complexity of the phase change condensation inside the Laval nozzle and the diversity of the influencing factors, the location of the excitation wave caused by the high-speed flow of hydrogen in the Laval nozzle and the influence of the excitation wave on the droplet condensation are not yet clear and need to be further investigated.

Declaration of Interest

We declare that we have no financial and personal relationships with other people or organizations that can inappropriately influence our work, there is no professional or other personal interest of any nature or kind in any product, service and/or company that could be construed as influencing the position presented in, or the review of the manuscript entitled.

Acknowledgements

This study is supported by the National Natural Science Foundation of China (U2241257), the Postdoctoral Science Foundation of China (2022M723497).

Nomenclature

dr/dt	droplet growth rate of ammonia, $m\cdot s^{-1}$
E	the total energy, J
h_{lv}	latent heat of condensation, $J\cdot kg^{-1}$
J	nucleation rate, $m^{-3}\cdot s^{-1}$
Kn	heat transfer coefficient between hydrogen molecules and condensed liquid droplets, $W\cdot m^{-2}\cdot K^{-1}$
Kr	heat transfer coefficient
k	turbulent kinetic energy, J
k_B	Boltzmann constant
L	length of tapering section, mm
m_o	mass of single molecule, g
N	droplet number per mass of gas, kg^{-1}
Pr_v	Prandtl number
p	pressure, Pa
q	heat flux, $W\cdot m^{-2}$
R	radius of section at any axial distance x, mm
R_M	gas constant
r	the grid refinement factor
r_{cr}	radius of throat section, mm
r_d	droplet radius, m
S	supersaturation
S_h	source term of vapor energy equation, $J\cdot m^{-3}\cdot s^{-1}$
S_m	source term of vapor continuity equation, $J\cdot m^{-3}\cdot s^{-1}$
S_u	source term of vapor momentum equation, $J\cdot m^{-2}\cdot s^{-2}$
S_Y	source term of liquid continuity equation, $J\cdot m^{-3}\cdot s^{-1}$
T	temperature, K
ΔT	subcooling degree, K
T_s	saturation temperature of vapor, K
t	time, s
u	velocity, $m\cdot s^{-1}$
x, y	Cartesian coordinates
Y	mass fraction of liquid phase
γ	the specific heat ratio of the vapor phase
λ_v	thermal conductivity of the vapor, $W\cdot m^{-1}\cdot K^{-1}$
ρ_l	density of liquid, $kg\cdot m^{-3}$
ρ_v	density of vapor, $kg\cdot m^{-3}$
θ	dimensionless surface tension
τ_{ij}	effective stress tensor
σ	droplet surface tension, $N\cdot m^{-1}$
ω	specific dissipation rate, %

Subscripts

i	x axis
j	y axis
l	liquid phase
v	vapor phase

References

[1] A. Shabanpour-Haghighi, M. Karimaghaei, An overview on multi-carrier energy networks: From a concept to future trends and challenges, *Int. J. Hydrogen Energy* 47 (9) (2022) 6164–6186.
[2] M. Aziz, Liquid hydrogen: A review on liquefaction, storage, transportation, and safety, *Energies* 14 (18) (2021) 5917.
[3] H. Li, X.W. Cao, Y. Liu, Y.B. Shao, Z.L. Nan, L. Teng, W.S. Peng, J. Bian, Safety of hydrogen storage and transportation: An overview on mechanisms, techniques, and challenges, *Energy Rep.* 8 (2022) 6258–6269.
[4] O. Faye, J. Szpunar, U. Eduok, A critical review on the current technologies for the generation, storage, and transportation of hydrogen, *Int. J. Hydrogen Energy* 47 (29) (2022) 13771–13802.
[5] X.W. Cao, J. Bian, Supersonic separation technology for natural gas processing: A review, *Chem. Eng. Process. Process. Intensif.* 136 (2019) 138–151.
[6] C. Wen, X.W. Cao, Y. Yang, J. Zhang, Supersonic swirling characteristics of natural gas in convergent-divergent nozzles, *Petrol. Sci.* 8 (1) (2011) 114–119.
[7] C. Wen, H.B. Ding, Y. Yang, Numerical simulation of nanodroplet generation of water vapour in high-pressure supersonic flows for the potential of clean natural gas dehydration, *Energy Convers. Manag.* 231 (2021) 113853.
[8] F. Frankl, To the theory of the Laval nozzle, *Izv. Akad. Nauk SSSR Ser. Mat.* 9 (1945) 387–422.
[9] J.N. Chen, Z. Huang, Numerical study on carbon dioxide capture in flue gas by converging-diverging nozzle, *Fuel* 320 (2022) 123889.
[10] J.N. Chen, Z. Huang, Spontaneous condensation of carbon dioxide in flue gas at supersonic state, *Energy* 254 (2022) 124418.
[11] J.N. Chen, Z. Huang, A.N. Li, R. Gao, W.M. Jiang, Carbon capture in Laval nozzles with different bicubic parametric curves and translation of witoszynski curves, *Energy* 260 (2022) 125144.
[12] Y. Liu, X.W. Cao, D. Guo, H.G. Cao, J. Bian, Influence of shock wave/boundary layer interaction on condensation flow and energy recovery in supersonic nozzle, *Energy* 263 (2023) 125662.
[13] Y. Liu, X.W. Cao, J. Yang, Y.X. Li, J. Bian, Energy separation and condensation effects in pressure energy recovery process of natural gas supersonic dehydration, *Energy Convers. Manag.* 245 (2021) 114557.
[14] H. Pathak, K. Mullick, S. Tanimura, B.E. Wyslouzil, Nonisothermal droplet growth in the free molecular regime, *Aerosol Sci. Technol.* 47 (12) (2013) 1310–1324.
[15] J. Bian, W.M. Jiang, L. Teng, Y. Liu, S.W. Wang, Z.F. Deng, Structure improvements and numerical simulation of supersonic separators, *Chem. Eng. Process. Intensif.* 110 (2016) 214–219.
[16] J. Bian, Y. Liu, X.H. Zhang, Y.F. Li, L. Gong, X.W. Cao, Co-condensation and interaction mechanism of acidic gases in supersonic separator: A method for simultaneous removal of carbon dioxide and hydrogen sulfide from natural gas, *Sep. Purif. Technol.* 322 (2023) 124296.
[17] X.W. Cao, W. Yang, Numerical simulation of binary-gas condensation characteristics in supersonic nozzles, *J. Nat. Gas Sci. Eng.* 25 (2015) 197–206.
[18] X.W. Cao, X.D. Song, Q. Chu, L.S. Mu, Y.X. Li, J. Bian, An efficient method for removing hydrogen sulfide from natural gas using supersonic Laval nozzle, *Process. Saf. Environ. Prot.* 129 (2019) 220–229.
[19] J.N. Chen, A.N. Li, Z. Huang, W.M. Jiang, G. Xi, Effect of shock wave on nucleation and droplet growth of CO_2 in flue gas in supersonic separators, *Gas Sci. Eng.* 113 (2023) 204975.
[20] Y. Liu, C.C. Wang, J.P. Wei, C.J. Chen, Effect of nozzle pressure ratio on pulsation frequency of air jets used in hole drilling, *J. Petrol. Sci. Eng.* 196 (2021) 107399.
[21] Y. Yang, J.H. Walther, Y.Y. Yan, C. Wen, CFD modeling of condensation process of water vapor in supersonic flows, *Appl. Therm. Eng.* 115 (2017) 1357–1362.
[22] C. Wen, H.B. Ding, Y. Yang, Optimisation study of a supersonic separator considering nonequilibrium condensation behaviour, *Energy Convers. Manag.* 222 (2020) 113210.
[23] H.B. Ding, Y. Zhang, Y.Y. Dong, C. Wen, Y. Yang, High-pressure supersonic carbon dioxide (CO_2) separation benefiting carbon capture, utilisation and storage (CCUS) technology, *Appl. Energy* 339 (2023) 120975.
[24] H.B. Ding, Y. Zhang, C.Q. Sun, Y. Yang, C. Wen, Numerical simulation of supersonic condensation flows using Eulerian-Lagrangian and Eulerian wall film models, *Energy* 258 (2022) 124833.
[25] C.Y. Han, W.M. Jiang, Y. Liu, Z.Z. Hu, Z.Y. Dou, Numerical simulation study on the structure optimization of liquid separation device in supersonic separator, *Sep. Sci. Technol.* 58 (4) (2023) 789–808.
[26] J. Bian, X.W. Cao, W. Yang, M.A. Edem, P.B. Yin, W.M. Jiang, Supersonic liquefaction properties of natural gas in the Laval nozzle, *Energy* 159 (2018) 706–715.
[27] G. Gyarmathy, The spherical droplet in gaseous carrier streams: Review and synthesis, *Multiph. Sci. Technol.* 1 (1–4) (1982) 99–279.
[28] J. Bian, X.W. Cao, W. Yang, H. Du, P.B. Yin, Effects of external particles on the liquefaction property of natural gas in a Laval nozzle, *Powder Technol.* 339 (2018) 894–902.
[29] National Institute of Standards and Technology, NIST chemistry WebBook. http://webbook.nist.gov/chemistry/, 2011. (Accessed 27 May 2018).
[30] S.H.R. Shooshtari, A. Shahsavand, Maximization of energy recovery inside supersonic separator in the presence of condensation and normal shock wave, *Energy* 120 (2017) 153–163.
[31] X.W. Liu, Z.L. Liu, Numerical investigation and improvement strategy of flow characteristics inside supersonic separator, *Sep. Sci. Technol.* 53 (6) (2018) 940–952.
[32] D.Y. Hou, W.M. Jiang, W.X. Zhao, J. Bian, Y. Liu, X.Y. Lai, Effect of linetype of convergent section on supersonic condensation characteristics of CH_4-CO_2 mixture gas in Laval nozzle, *Chem. Eng. Process. Process. Intensif.* 133 (2018) 128–136.
[33] C.Y. Han, W.M. Jiang, Y. Liu, Z.Y. Dou, B.X. Jin, Numerical study on carbon dioxide removal from the hydrogen-rich stream by supersonic Laval nozzle, *Int. J. Hydrogen Energy* 48 (38) (2023) 14299–14321.
[34] C.A. Moses, G.D. Stein, On the growth of steam droplets formed in a Laval nozzle using both static pressure and light scattering measurements, *J. Fluids Eng.* 100 (3) (1978) 311–322.